INTERNATIONAL JOURNAL OF RESEARCH AND SCIENTIFIC INNOVATION (IJRSI)
ISSN No. 2321-2705 | DOI: 10.51244/IJRSI |Volume XIII Issue I January 2026

# AI-Driven Environmental Pollution Detection Using Zinc Oxide Nanoparticles Synthesized from *Ulva Intestinalis*

**Keerthanaa Vijayanand[1], Raghul Rajah Santha Moorthi Rajah[2], Aakash Sumesh Kumar[2]**

**[1]BITS PILANI, Pilani**

**[2]Sathyabama Institute of Science and Technology, Chennai**

**DOI: https://doi.org/10.51244/IJRSI.2026.13010075**

**Received: 14 January 2026; Accepted: 19 January 2026; Published: 31 January 2026**

## ABSTRACT

Ulva-mediated green synthesis of zinc oxide (ZnO) nanomaterials offers a sustainable pathway for next-generation environmental monitoring platforms that overcome the limitations of conventional laboratory-bound pollutant analysis. This review critically examines the role of *Ulva intestinalis* as a biofactory for ZnO nanoparticles and connects its unique phytochemical profile to mechanistic aspects of nanoparticle formation, surface functionalization, and performance in sensing applications. The discussion begins with the changing global pollution landscape and the constraints of chromatographic–mass spectrometric techniques, motivating a shift toward distributed nanosensor systems capable of real-time detection of complex contaminant mixtures. The principles of green chemistry are then related to *Ulva*-derived extracts, highlighting how ulvan, proteins, and associated polysaccharides act as reducing, chelating, and capping agents that drive nucleation, growth, and stabilization of wurtzite-phase ZnO with tailored morphology, porosity, and surface chemistry. Subsequent sections link physicochemical features such as crystal structure, defect states, bandgap, and bio-organic corona to chemiresistive gas sensing, photocatalytic degradation, and electrochemical detection of heavy metal ions in environmental matrices. Particular emphasis is placed on the integration of artificial intelligence and machine learning for signal preprocessing, feature extraction, pattern recognition, and drift compensation, supporting robust pollutant classification and quantification under variable humidity and multi-pollutant conditions. Finally, the review outlines the incorporation of green-synthesized ZnO into IoT and AIoT architectures, addressing biosafety, ecotoxicological considerations, scalability of algal synthesis, and prospects for self-powered piezo-phototronic devices within smart environmental monitoring ecosystems.

**Keywords :** *Ulva intestinalis*, green synthesis, zinc oxide nanoparticles, environmental pollution, chemiresistive sensing, artificial intelligence, machine learning, IoT, AIoT.

## INTRODUCTION

Environmental monitoring has moved from simple pollutant tracking to complex, data-driven assessment of ecosystem health [1,2]. This evolution reflects rapid industrialization, urban growth, and the spread of new chemical classes that place pressure on air, water, and soil quality [3].

### Global Pollution Landscape

The current pollution landscape is dominated by diverse contaminants that act at low concentrations and persist in the environment. These include persistent organic pollutants, pharmaceuticals, personal care products, pesticides, heavy metals, and emerging classes such as endocrine-disrupting compounds and microplastics [4]. Many of these substances occur as complex mixtures in environmental matrices, which complicates risk assessment and regulatory monitoring. Monitoring gaps arise when analytical methods target a narrow set of known pollutants while unmonitored transformation products or novel contaminants remain undetected [5]. Diffuse pollution sources, such as urban runoff and agricultural drainage, further reduce the effectiveness of conventional surveillance networks that were designed for point sources [2].

**Limitations of Conventional Analytical Techniques**

Gas chromatography–mass spectrometry and high-performance liquid chromatography with mass spectrometric detection are standard tools for environmental analysis. These techniques provide high selectivity, low detection limits in the sub-nanogram per litre range, and robust quantification for many organic contaminants [4]. They also support method validation, quality assurance, and regulatory acceptance across water, sediment, and biota samples. Despite these strengths, GC-MS and HPLC workflows rely on laborious sample preparation steps such as extraction, concentration, and clean-up that increase cost and turnaround time. Matrix effects and instrument sensitivity constraints limit performance when very low concentrations or highly complex samples are analysed [6]. Routine methods usually monitor predetermined analytes, so unknown or structurally diverse emerging contaminants are often missed. Traditional systems are also centralized in laboratories, which restricts spatial and temporal coverage and reduces responsiveness during pollution incidents. [5]

**Shift to Real-Time Intelligent Sensing**

These limitations have encouraged a move from offline laboratory assays toward distributed sensing platforms that operate close to the contamination source. Advances in nanomaterials, including zinc oxide nanostructures, have enabled compact sensors with high surface area, tailored surface chemistry, and strong photocatalytic or electrochemical responses to pollutants [7]. ZnO-based sensing elements can detect gases, organic dyes, antibiotics, and other solutes through changes in conductivity, optical signals, or catalytic degradation profiles [8].

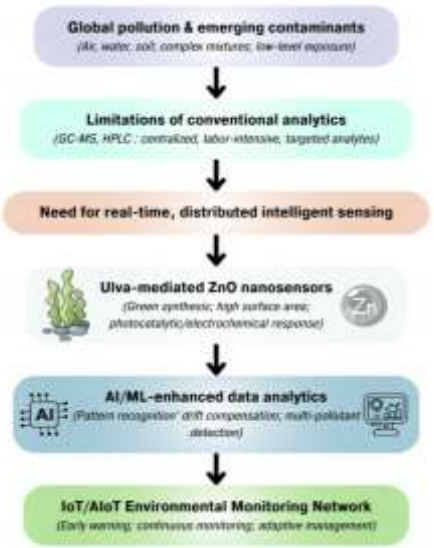


Fig. 1. Conceptual workflow illustrating Ulva-mediated ZnO nanoparticle synthesis integrated with AI-driven environmental sensing pipelines.

**Commented [K1]:** *Fig. 1. Conceptual workflow illustrating Ulva-mediated ZnO nanoparticle synthesis integrated with AI-driven environmental sensing pipelines.*

Green synthesis routes that use marine algae of the Ulva genus as reducing and stabilizing agents provide biogenic ZnO nanoparticles with photocatalytic and antimicrobial activity while reducing synthetic toxicity and cost [9]. Machine learning and broader artificial intelligence methods now support pattern recognition in complex spectral or sensor datasets, which allows classification and quantification of multiple pollutants from a single sensor response [10]. Integrating AI models with nanostructured ZnO sensors enables real-time decision support for water treatment, early warning systems, and adaptive environmental management strategies [11].

**Nanotechnology in Next-Generation Sensing**

Nanotechnology has transformed chemical sensing by providing materials with tunable structure, high reactivity, and strong signal transduction at very small scales. Nanosensors now support trace-level detection, rapid response, and miniaturized platforms that can integrate with electronic and optical readout systems [12,13].

**Physicochemical Advantages of Nanomaterials.**

Nanomaterials exhibit a very high surface-to-volume ratio, which increases the number of active sites available for adsorption and interfacial reactions. This feature enhances sensitivity, because a larger fraction of atoms resides at or near the surface and can interact with target analytes. The high surface area also improves catalytic activity, charge transfer, and mass transport properties that are important for chemical and biosensing applications [14]. When particle dimensions approach the exciton Bohr radius, quantum confinement modifies electronic band structures and leads to size-dependent optical and electronic properties. Quantum dots and other quantum-confined systems can show discrete energy levels, shifted absorption and emission spectra, and enhanced fluorescence, which are useful for optical sensing and signal amplification [15]. These physicochemical effects allow nanoscale materials to achieve stronger, more selective transduction of chemical events than their bulk counterparts [16].

**Metal oxide semiconductors as chemiresistive layers**

Semiconducting metal oxides are widely used as chemiresistive sensing layers because their electrical resistance changes with gas or analyte exposure [17]. Typical materials include ZnO, $SnO_2$, $TiO_2$, $WO_3$, and related oxides that operate through adsorption of oxygen species and subsequent charge transfer with target molecules. Interaction of oxidizing or reducing gases with surface oxygen alters the concentration of charge carriers in the depletion layer, which produces a measurable resistance change [18]. Nanostructured MOS films, such as nanoparticles, nanowires, and porous architectures, provide large accessible surface area and interconnected pathways that enhance sensitivity and response speed. These sensors offer simple device architecture, compatibility with microfabrication, and relatively low manufacturing cost, which supports deployment in dense monitoring networks [19]. Key challenges involve selectivity, humidity dependence, and the need for elevated operating temperatures, although strategies such as doping, heterojunction formation, and light activation are improving performance [20].

**Rationale for zinc oxide in sensing**

Zinc oxide is a II–VI semiconductor with a wide direct bandgap and large exciton binding energy that supports robust optical and electronic responses at room temperature. It can be synthesized in diverse morphologies, including nanorods, nanowires, nanosheets, and quantum dots, which allows control over surface area, porosity, and charge transport pathways [21]. ZnO shows good chemical stability, non-toxic or low-toxic behaviour in many applications, and biocompatibility that is suitable for biosensing and environmental monitoring. In optical sensing, ZnO nanostructures act as efficient platforms for photoluminescence, fluorescence enhancement, and waveguiding, which supports label-free and labelled detection schemes [22]. In electrochemical and chemiresistive sensors, ZnO offers high isoelectric point, fast electron transfer, and strong adsorption of various analytes, which improves sensitivity and lowers detection limits for gases, small molecules, and biomolecules [23]. These combined optical and electrochemical capabilities make ZnO a versatile base material for next-generation hybrid sensors that couple different transduction modes and interface readily with AI-driven data analysis [24,25].

***Ulva intestinalis*-Mediated Green Synthesis of ZnO**

Green synthesis of zinc oxide nanomaterials uses biological extracts to replace harsh chemical reagents and high-energy processes [26]. *Ulva intestinalis* fits this approach because its cell wall polysaccharides and associated biomolecules can act as reducing, chelating, and stabilizing agents during nanoparticle formation [27].

**Green chemistry principles in nanotechnology**

Green chemistry in nanomaterial synthesis aims to minimize toxic reagents, waste generation, and energy consumption while maintaining control over particle properties. Biological routes use plant, algal, microbial, or waste-derived extracts to reduce metal precursors and cap the growing nanocrystals [28]. These methods often proceed in aqueous media, operate at mild temperature and pressure, and avoid strong organic solvents or hazardous reducing agents such as hydrazine and sodium borohydride. Reports on green synthesis of ZnO nanoparticles highlight low cost, improved safety, and better environmental compatibility compared with conventional physical and chemical routes [29]. At the same time, the presence of biomolecules on the nanoparticle surface can enhance dispersibility and biocompatibility, which benefits sensing and biomedical applications [30].

**Phytochemical profile and functional role of Ulva intestinalis**

Ulva species contain a distinctive sulphated polysaccharide, ulvan, together with cellulose, xyloglucans, glucuronans, proteins, and minor phenolic compounds [31]. Ulvan contributes between roughly one tenth and one third of the dry biomass and is mainly composed of sulphated rhamnose and uronic acid units that present abundant hydroxyl, carboxyl, and sulphate groups [32]. These functional groups can bind metal ions, donate electrons, and participate in nucleation and growth processes during nanoparticle synthesis. Seaweed extracts of Ulva and related green macroalgae also contain water-soluble proteins, peptides, and other polysaccharides, whose amine, carboxyl, and hydroxyl groups contribute to metal ion complexation and act as capping shells around nascent particles [33]. Studies using *Ulva lactuca*, *Ulva fasciata*, and other Ulva species for ZnO nanoparticle synthesis show that these biomolecules are responsible for both reduction and stabilization, as demonstrated by characteristic bands in FTIR spectra associated with polysaccharides and proteins [9,11].

**Mechanism of ZnO formation with Ulva extracts**

The formation mechanism of Ulva-mediated ZnO nanoparticles involves a sequence of chelation, reduction, and stabilization steps at the molecular level. First, zinc ions from salts such as zinc acetate or zinc nitrate coordinate with hydroxyl, carboxylate, sulphate, and amino groups present on ulvan chains and associated biomolecules, which creates metal–polymer complexes in solution [9,34]. Under suitable pH and temperature, deprotonated hydroxyl and carboxyl groups promote hydrolysis of the metal precursor and formation of zinc hydroxide or oxyhydroxide intermediates. Subsequent dehydration and rearrangement yield crystalline ZnO nuclei that grow into nanoparticles or other nanostructures [26].


Fig. 2. Mechanistic flow of Ulva-mediated green ZnO synthesis

Throughout this process, ulvan and other macromolecules adsorb on particle surfaces and form a capping layer that limits aggregation, controls growth directions, and stabilizes the colloidal dispersion. Spectroscopic evidence from FTIR and UV–Vis measurements in algal ZnO systems supports the involvement of polysaccharide and protein functional groups in both reduction and capping activities [30,35].

**Comparative aspects of Ulva intestinalis versus other synthesis routes**

Algal-mediated synthesis using Ulva species offers several advantages compared with conventional chemical methods and other biological platforms. Ulva biomass is abundant, grows rapidly in marine and coastal environments, and can be cultivated or harvested from blooms, which supports low-cost and renewable precursor supply [36]. The process usually runs at moderate temperatures in water, with no need for pressurized reactors

or high-temperature calcination steps used in many solid-states or sol–gel syntheses, which improves energy efficiency [28]. Reports on Ulva-based ZnO nanoparticles describe hexagonal wurtzite structures with particle sizes in the tens of nanometres and relatively narrow distributions, which indicates reasonable morphology control through adjustment of extract concentration, pH, and reaction time [11]. Compared with microalgal systems such as Arthrospira or Spirogyra, Ulva extracts provide high polysaccharide content and strong metal-binding capacity that can promote rapid nucleation and effective capping, although reaction rates and final purity can vary with seasonal and geographic changes in biomass composition [36]. Chemical syntheses based on high-temperature precipitation, combustion, or hydrothermal routes often yield highly crystalline ZnO with tight control over size and shape, but they rely on toxic precursors, higher energy inputs, and post-synthetic surface modification, whereas Ulva-mediated routes integrate synthesis and functional surface coating in a single, more sustainable step [26].

**Physicochemical Characterization & Functional Assessment**

Physicochemical characterization of Ulva-mediated ZnO focuses on establishing crystal structure, morphology, surface area, optical response, and surface chemistry of the bio-capped nanoparticles. These properties govern dispersion stability, bandgap, and adsorption behaviour, which together determine suitability for sensing and environmental applications [11].

## MORPHOLOGY, STRUCTURE, AND SURFACE AREA

X-ray diffraction confirms phase purity and crystallinity of green-synthesized ZnO nanoparticles. Studies using Ulva and other seaweed extracts typically report diffraction peaks that match the hexagonal wurtzite structure, with Debye–Scherrer analysis giving crystallite sizes in the nanometre range [37]. The absence of extra peaks indicates that residual inorganic impurities or secondary zinc phases are minimal under optimized synthesis conditions [38].

Electron microscopy provides direct insight into particle size, shape, and aggregation state. SEM images of algal-derived ZnO often show quasi-spherical, rod-like, or flower-like assemblies formed by smaller primary nanoparticles, reflecting the templating effect of biomolecules during growth. TEM and selected area electron diffraction confirm nanoscale dimensions and crystalline lattice fringes that align with wurtzite ZnO planes [39]. BET surface area analysis of green ZnO usually reveals moderate to high specific surface areas and micro- or mesoporous textures, which increase the density of adsorption sites and enhance catalytic or sensing performance. Pore size distributions and total pore volume give further information on accessibility of internal surfaces and diffusion pathways for pollutant molecules [38,40].

Table 1. Summary of physicochemical characterization techniques used for Ulva-mediated ZnO nanoparticles and their relevance to environmental sensing applications [37-40].

Commented [K2]: Chk if it is needed

| Technique | Information obtained | Relevance to sensing performance |
|---|---|---|
| XRD | Crystal phase, crystallinity, crystallite size | Determines charge transport efficiency and defect-related sensing behaviour |
| SEM / TEM | Particle size, morphology, aggregation | Influences surface reactivity, adsorption kinetics, and sensitivity |
| BET analysis | Surface area, porosity | Governs density of active adsorption sites and response magnitude |
| FTIR | Functional groups, bio-capping molecules | Confirms surface chemistry and pollutant–surface interactions |

| | | |
|---|---|---|
| UV–Vis spectroscopy | Optical absorption edge, bandgap | Relevant for optical sensing and photocatalytic activation |
| Photoluminescence (PL) | Defect states, recombination pathways | Correlates with oxygen vacancies and chemiresistive response |

**Optical properties and bandgap features**

UV–Vis spectroscopy is a key tool to verify nanoparticle formation and estimate optical bandgap. Green ZnO systems commonly display a strong absorption edge or excitonic peak in the near-UV region, typically around 360–380 nm, which is characteristic of ZnO nanostructures [37]. The position of this absorption edge can shift slightly with particle size, defect concentration, and surface capping, which reflects quantum-size effects and band structure modification at the nanoscale [27].

Tauc plot analysis of UV–Vis data gives bandgap energies that often lie close to or slightly above the bulk ZnO value, consistent with nanoscale crystallites and surface strain [37]. Photoluminescence measurements reveal near-band-edge emission in the UV and broad visible bands associated with oxygen vacancies and other intrinsic defects [41]. The relative intensity and position of these PL features provide information on defect density and surface states, which are important for photocatalysis and optical sensing because they govern charge carrier recombination and trapping. Control over synthesis parameters and biomass concentration allows partial tuning of bandgap and defect-related emission, which can be exploited to optimize light absorption and signal transduction in sensor designs [42].

**Surface chemistry and FTIR evidence for bio-capping**

Fourier transform infrared spectroscopy is used to probe organic functional groups associated with Ulva-derived capping agents on ZnO surfaces. FTIR spectra of green-synthesized ZnO typically show broad bands in the region of O–H and N–H stretching, along with peaks corresponding to C=O, C–N, S=O, and C–O vibrations that originate from ulvan, other polysaccharides, proteins, and minor metabolites [9]. A distinct band in the low-wavenumber region, often between about 400 and 600 $cm^{-1}$, is assigned to Zn–O stretching and confirms successful nanoparticle formation [27].

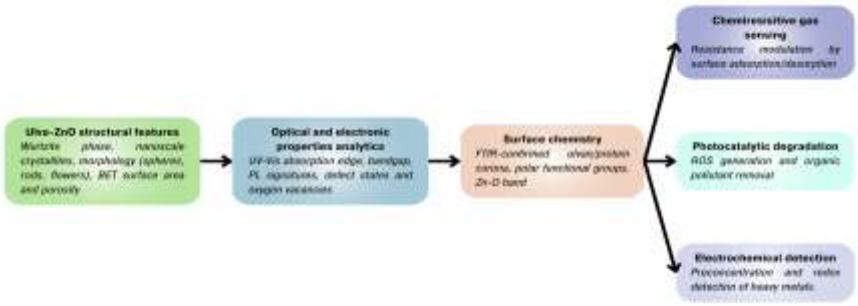


Fig. 3. Structure–property–function pathway of Ulva-ZnO

Comparison of FTIR spectra for crude Ulva extract and the corresponding ZnO nanoparticles shows shifts or intensity changes in key bands, which indicates coordination of zinc ions with hydroxyl, carboxylate, sulphate, and amino groups during synthesis. These interactions produce a bio-organic corona that stabilizes the colloid, limits aggregation, and introduces hydrophilic functional groups at the particle surface [43]. The abundance of polar groups on the capped ZnO surface enhances adsorption of ionic and polar pollutants, supports hydrogen bonding and electrostatic interactions, and can improve affinity for dyes, metals, or biomolecules in sensing and

remediation applications. FTIR analysis before and after adsorption experiments often reveals changes in band positions or intensities, which provides mechanistic insight into how specific functional groups participate in binding and removal of contaminants [37,40].

**Sensing Mechanisms and Transduction**

Chemiresistive, photocatalytic, and electrochemical pathways provide complementary routes for converting physicochemical interactions at ZnO surfaces into measurable signals. These mechanisms rely on oxygen vacancies, bandgap-driven excitations, and interfacial charge transfer, which are strongly influenced by nanostructure morphology and surface chemistry [20].

**Chemiresistive gas sensing**

Chemiresistive ZnO sensors operate through modulation of electrical resistance by gas adsorption at the surface. In air, oxygen molecules adsorb on ZnO and capture conduction-band electrons to form negatively charged species such as $O_2^-$, $O^-$, and $O^{2-}$, which generate an electron-depletion layer near the surface [20]. This depletion region increases the potential barrier at grain boundaries and reduces conductivity in n-type ZnO [44]. Intrinsic oxygen vacancies act as donor states and preferential adsorption sites, so a higher vacancy concentration increases baseline electron density but also raises the density of reactive surface sites [45].

Exposure to a reducing gas leads to reaction with adsorbed oxygen species and releases trapped electrons back into the conduction band. The depletion layer becomes thinner, the barrier height decreases, and the sensor resistance drops. Oxidizing gases withdraw additional electrons or form new surface complexes, which thickens the depletion layer and increases resistance [20]. The magnitude and dynamics of these resistance changes depend on defect chemistry, grain size, porosity, operating temperature, and the presence of dopants or heterojunctions that tailor oxygen vacancy populations and charge transport [46].

**Photocatalytic degradation and ROS generation**

ZnO photocatalysis is driven by bandgap excitation and subsequent formation of reactive oxygen species that oxidize organic pollutants. Under UV or suitable visible irradiation, photons with energy equal to or greater than the ZnO bandgap generate electron–hole pairs, with electrons promoted to the conduction band and holes left in the valence band. Efficient separation and migration of these charge carriers to the surface are critical for catalytic activity because rapid recombination wastes the absorbed energy [47].

At the surface, photogenerated holes can oxidize adsorbed water or hydroxide ions to produce hydroxyl radicals, while conduction-band electrons reduce dissolved oxygen to superoxide species. Subsequent reactions yield additional ROS, including - OH, $O_2^-$- , and related oxidants that attack chromophoric bonds and functional groups in dyes, phenols, and other organic contaminants, eventually mineralizing them to carbon dioxide and water [48]. Particle size, defect density, and surface area influence light absorption, carrier diffusion lengths, and ROS generation efficiency [49]. Composites and doped ZnO structures can extend the absorption edge, suppress recombination, and enhance degradation rates under solar or low-intensity light [50,51].

**Electrochemical detection of heavy metal ions**

In electrochemical sensors, ZnO nanostructures act as active interfaces that preconcentrate metal ions and facilitate electron transfer during redox processes. ZnO coatings on electrodes such as glassy carbon, indium tin oxide, or carbon paste increase effective surface area and provide hydroxyl-rich, polar surfaces that coordinate with cationic metal species. Adsorption occurs through electrostatic attraction, Lewis acid–base interactions, and complexation with surface –OH and defect sites, which enhances local analyte concentration prior to the electrochemical step [52,53].

Techniques such as anodic stripping voltammetry and differential pulse voltammetry are commonly used for detection. During a pre-deposition step at negative potential, target heavy metal ions are reduced and accumulate on the modified electrode surface, sometimes forming alloys with auxiliary metals such as bismuth. A

subsequent anodic scan re-oxidizes the deposited metals, producing current peaks whose height is proportional to concentration [53,54]. ZnO morphology plays a central role, with porous nanoplates, nanotubes, and hierarchical architectures showing higher sensitivity than dense nanorods, due to greater surface-to-volume ratio and more accessible adsorption sites [52]. Coupling ZnO with conductive supports such as graphene or carbon nanotubes further improves charge transfer kinetics and lowers detection limits for ions such as $Pb^{2+}$, $Cd^{2+}$, and $Hg^{2+}$ in complex water matrices [55,56].

**Challenges in ZnO Sensing: The Need for AI**

Selectivity, long-term stability, and signal interpretation remain major bottlenecks for ZnO-based sensors, which motivates the integration of AI-driven data analysis and compensation strategies [57]. These issues are pronounced under variable humidity and in complex, multi-pollutant environments where traditional calibration models are not sufficient [6].

**Selectivity and cross-sensitivity**

ZnO chemiresistive sensors respond to many oxidizing and reducing gases, so the same material can exhibit similar resistance changes toward chemically different analytes. This broad reactivity produces cross-sensitivity, where interfering species or background gases contribute to the signal and compromise selectivity for the target pollutant [58]. Water vapor is a major interferent because adsorbed moisture alters surface chemistry, introduces protonic conduction pathways, and changes baseline resistance as relative humidity varies [59]. Even when material engineering strategies such as noble-metal decoration, heterojunction formation, or morphology tuning reduce humidity effects, selectivity problems are not fully removed [60]. AI-based pattern recognition can help distinguish gases by exploiting subtle differences in dynamic response profiles, recovery behaviour, and multi-sensor array outputs rather than relying on single steady-state resistance values [61,62].

**Hysteresis and baseline drift**

Long-term deployment exposes ZnO sensors to temperature cycles, fluctuating humidity, and repeated adsorption–desorption, which induce hysteresis and drift. Hysteresis arises when the sensor response during increasing gas concentration does not follow the same path as during decreasing concentration due to slow diffusion, incomplete desorption, or irreversible surface reactions. Baseline drift reflects gradual changes in sensor resistance over time in clean air, driven by aging of the sensing film, poisoning of active sites, grain boundary modifications, or mechanical and contact instabilities [63]. These effects reduce calibration accuracy and can mimic low-concentration pollutant events if not corrected [64]. AI and machine learning models can incorporate time-series information, identify drift patterns, and perform adaptive baseline correction or virtual recalibration using historical data, which stabilizes outputs over extended operation [65,66].

**Data complexity in multi-pollutant environments**

Real-world air and water matrices contain mixtures of gases and vapours at varying concentrations, which generate complex, overlapping response patterns across sensor arrays. The raw data are often high-dimensional and non-linear, because each sensor channel depends on concentration, temperature, humidity, and exposure history. Simple threshold-based or univariate calibration approaches cannot separate contributions from multiple pollutants under such conditions [67,68]. AI methods, including principal component analysis, support vector machines, and deep learning models such as LSTM or fully convolutional networks, can extract discriminative features from transient and steady-state responses and classify or quantify multiple species simultaneously [57,62]. These algorithms also support sensor fusion, where data from ZnO chemiresistive, optical, and electrochemical channels are integrated to improve robustness against cross-sensitivity and to provide richer, context-aware pollution assessment [67,69].

**Artificial Intelligence and Machine Learning Integration**

Artificial intelligence augments ZnO-based sensing by transforming complex, noisy signals into reliable information about pollutant identity and concentration. Signal processing, pattern recognition, and drift compensation form an integrated pipeline that links the material response to robust environmental data [69].

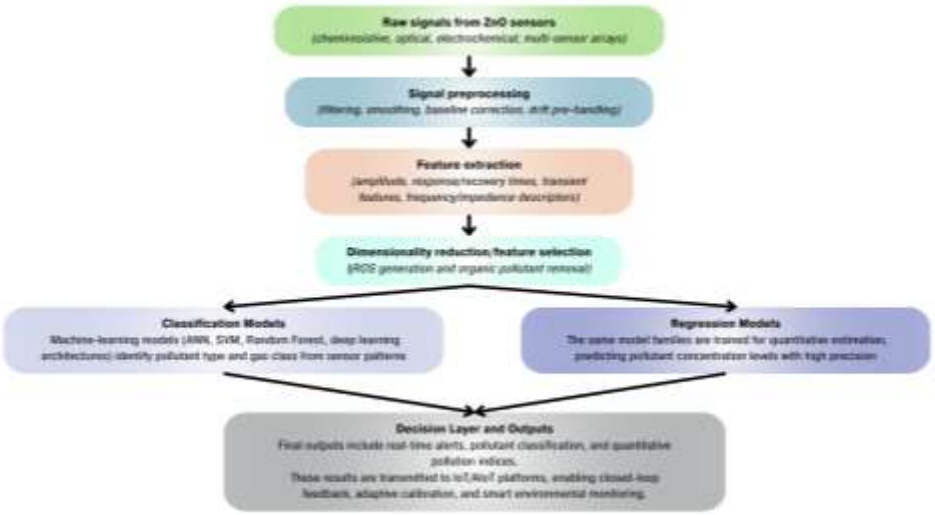


Fig. 4. AI pipeline for processing ZnO sensor signals

**Signal processing and feature extraction**

Raw outputs from chemiresistive, optical, or electrochemical ZnO sensors often contain noise, baseline fluctuations, and transient artifacts. Preprocessing commonly applies filtering, smoothing, and baseline correction to improve signal-to-noise ratio while preserving relevant response dynamics. Features are then extracted to summarize sensor behaviour, such as response amplitude, response and recovery rates, area under the response curve, steady-state values, and selected time points or frequency components [62]. These features reduce dependence on raw time-series while capturing both kinetic and equilibrium aspects of gas–sensor interactions [70].

Dimensionality reduction techniques handle the high dimensionality that arises from multi-sensor arrays and rich feature sets. Principal component analysis projects the feature space onto orthogonal directions that retain most of the variance, which simplifies visualization, mitigates collinearity, and filters noise. Linear discriminant analysis, a supervised approach, further seeks projections that maximize class separation between different gases or concentrations, often improving classification performance compared with PCA alone. These reduced representations serve as compact inputs for downstream classifiers and regressors [62,71].

**Pattern recognition with ANN, SVM, and Random Forest**

Pattern recognition algorithms learn the mapping from processed sensor features to gas identity or concentration. Artificial neural networks can approximate complex, nonlinear relationships in sensor data, which is useful when responses depend simultaneously on analyte type, mixture composition, temperature, and humidity. Single-hidden-layer and deep ANN architectures have been applied to classify volatile organic compounds and to predict concentrations from impedance or resistance spectra of ZnO-based sensors [72,73].

Support vector machines construct decision boundaries with good generalization in high-dimensional feature spaces and perform well on relatively small datasets. SVM classifiers have been used to discriminate among multiple VOCs and gas mixtures, while SVM regressors support quantitative analysis of concentrations [62]. Random Forest algorithms operate as ensembles of decision trees and handle nonlinearities, feature interactions, and heterogeneous noise [73]. They have been employed to classify gas types and to rank feature importance, which helps identify the most informative aspects of ZnO sensor responses. Comparative studies show that

combinations such as PCA or feature selection followed by SVM, ANN, or Random Forest can achieve high accuracy in multi-gas classification and quantification tasks [74].

**AI-enabled drift compensation**

Sensor aging and environmental fluctuations introduce drift that degrades performance over months of operation. AI-based drift compensation methods learn relationships between current sensor responses and historical patterns, allowing correction without frequent physical recalibration [75]. Some approaches extract intrinsic features that remain invariant to drift and then apply classification with models such as SVM, which improves long-term accuracy on multi-month datasets [64]. Others use domain-adaptive neural networks or contrastive learning to align features from pre-drift and post-drift conditions and to maintain performance on new data distributions [76].

Online and semi-supervised algorithms can update model parameters as new labelled or partially labelled data arrive, which supports continuous adaptation in changing environments [75,77]. Techniques such as ensemble CNNs and domain generalization frameworks combine predictions from multiple feature levels and penalize domain discrepancies to obtain robust outputs under drift [78,89]. These AI strategies extend the practical lifetime of ZnO-based sensing systems and help preserve calibration in real-world environmental monitoring deployments [70].

**Real-World Application: IoT and Smart Monitoring Ecosystems**

AIoT architectures allow ZnO-based sensors to operate as distributed, intelligent nodes that provide real-time environmental data and long-range analytics. Integration of edge computing, wireless communication, and cloud-based AI supports scalable deployment in air and water quality monitoring networks [57,80].

**AIoT environmental node architecture**

An AIoT environmental node typically combines sensing, computation, communication, and power subsystems in a layered architecture. At the device level, ZnO-based chemiresistive, optical, or electrochemical sensors interface with microcontrollers or low-power processors that perform signal conditioning, digitization, and on-device feature extraction. Edge computing units execute lightweight AI models for preliminary classification, anomaly detection, and event triggering, which reduces latency and lowers data volume sent to the cloud [81]. Wireless modules such as Wi-Fi, LoRaWAN, or cellular modems connect nodes to gateways and cloud platforms, where more complex machine learning, data fusion, and long-term drift analysis are carried out [1]. Power management relies on batteries, energy harvesting, and duty-cycling strategies to sustain continuous or near-continuous monitoring in remote locations [82].

**ZnO-based sensors in smart monitoring networks**

ZnO nanomaterials have been integrated into gas and chemical sensors that are suitable for networked deployment in air quality systems. La-doped ZnO chemiresistive sensors, for example, achieve room-temperature detection of $CO_2$ with high sensitivity and are described as compatible with IoT platforms for indoor air quality and building management [83]. Heterojunction devices such as ZnO/CuI UV-photovoltaic gas sensors provide self-powered operation while maintaining stable response, which is attractive for distributed wireless nodes [84]. Reviews on nano-enabled gas sensors highlight ZnO-based devices as candidates for smart city and industrial monitoring, where they can complement carbon-based and polymer sensors in hybrid IoT networks [85]. System-level studies of IoT and edge computing for environmental monitoring show that embedding machine learning at the edge reduces latency, bandwidth requirements, and energy consumption compared with cloud-only architectures. These findings support the use of ZnO sensor arrays as front-end transducers within AIoT frameworks that manage multi-pollutant detection across urban and industrial sites [1].

**Biosafety and ecotoxicology of green-synthesized ZnO**

Green-synthesized ZnO nanoparticles are often presented as safer alternatives to chemically produced analogues, yet ecotoxicological studies indicate that they can still induce adverse effects at elevated doses. Reviews of ZnO

nanoparticle toxicity report impacts on algae, plants, invertebrates, fish, and microorganisms that include oxidative stress, membrane disruption, and genotoxicity. Dissolution of ZnO and subsequent release of $Zn^{2+}$ ions play a central role in many toxicity mechanisms, with leaching rates depending on pH, ionic strength, and the presence of natural organic matter [86]. Experimental work with green-synthesized ZnO from plant extracts shows dose- and time-dependent toxicity in zebrafish embryos, with high concentrations causing increased mortality, delayed hatching, and developmental malformations, while concentrations below about 10 mg/L produce limited effects [87]. Surface coatings derived from biological capping agents can mitigate or modify toxicity by altering dissolution and interaction with biological interfaces, but they do not fully eliminate risk [88].

For environmental monitoring applications, biosafety assessment must therefore consider nanoparticle stability within sensor matrices, potential leaching from coatings or exposed films, and end-of-life disposal of sensing devices. Encapsulation of ZnO nanostructures in inert binders, use of robust substrates, and design of recovery and recycling schemes can reduce environmental release during operation [89]. Regulatory and risk assessment frameworks recommend a combination of in vitro assays, model organism tests, and environmental fate studies to evaluate chronic exposure scenarios for nano-enabled sensors, including those produced through green synthesis [86].

**Future Perspectives**

Large-scale algal synthesis and piezo-phototronic device concepts position ZnO as a core material for sustainable, intelligent, and potentially self-powered environmental sensors. Both directions require advances in process engineering, materials integration, and system-level design before widespread industrial deployment is possible [29].

**Scalability of algal synthesis**

Reviews of algal-mediated ZnO synthesis emphasize that marine macroalgae offer a renewable, non-food biomass source that does not compete for arable land or freshwater. Green seaweeds such as Ulva can be cultivated at scale in coastal farms and integrated into biorefinery concepts where polysaccharides, proteins, and pigments are fractionated for multiple product streams, including nanoparticle production [36]. The algal extract route to ZnO is attractive for industry because it operates in aqueous media at relatively low temperatures and uses low-cost equipment, which reduces energy demand and capital costs compared with high-temperature or vacuum-based methods [28].

At the same time, large-scale production faces challenges related to batch-to-batch variability in algal composition, process standardization, and product reproducibility. Seasonal, geographic, and processing differences alter ulvan and metabolite profiles, which affect reduction kinetics, particle size distributions, and surface chemistry of the resulting ZnO. Future work highlighted in recent reviews calls for controlled cultivation, upstream biomass conditioning, and inline monitoring of extract composition to improve consistency in nanoparticle quality [26]. Process intensification strategies such as continuous-flow reactors, membrane-assisted separations, and coupling of algal biorefineries with nanoparticle synthesis units are proposed to enhance throughput and enable integration into industrial sensor fabrication lines. For ZnO-based devices, scalable approaches will also need robust methods to deposit green-synthesized nanoparticles as inks, coatings, or patterned films that are compatible with printing, microfabrication, and packaging technologies [1,40].

**Towards self-powered piezo-phototronic ZnO sensors**

Piezo-phototronics exploits the coupling of piezoelectric polarization, semiconductor properties, and photoexcitation in ZnO and related materials to control charge transport and energy conversion [42]. When one-dimensional ZnO nanostructures such as nanowires or nanorods are mechanically deformed, internal piezoelectric potentials arise and modulate band structures at junctions, which can gate carriers in photodetectors, solar cells, and sensor interfaces. This three-field coupling enables devices where mechanical energy from vibrations, pressure, or environmental motions contributes directly to sensing or to auxiliary power generation [42,91].

Recent studies on ZnO-nanowire-based piezotronic and piezo-phototronic devices show enhanced responsivity and reduced power requirements in pressure sensors, photodetectors, and light-emitting systems [42]. Ordered arrays of vertically aligned ZnO nanowires, in particular, offer high piezopotential output and stable mechanical performance, which are advantageous for self-powered or low-power sensor platforms [92]. Concept papers and experimental demonstrations indicate that coupling ZnO nanogenerators or piezo-phototronic elements with gas or chemical sensing layers could yield hybrid devices where mechanical deformation and light both support signal amplification and partial energy harvesting [93]. Realization of practical self-powered environmental nodes will require reliable large-area growth or transfer of aligned ZnO structures, flexible and durable encapsulation, and efficient power management circuits that can store or directly use harvested energy in AIoT architectures [80].

## CONCLUSION

AI-enabled, Ulva-mediated ZnO nanosensing platforms represent a credible route toward continuous, context-aware environmental monitoring that overcomes the spatial, temporal, and analytical blind spots of conventional laboratory-based assays. By coupling the defect- and morphology-engineered wurtzite ZnO produced via green algal synthesis with multimodal chemiresistive, photocatalytic, and electrochemical transduction, this paradigm enables sensitive, low-footprint detection of complex pollutant mixtures across air and water matrices. Embedding these biogenic ZnO interfaces within AIoT architectures, supported by edge–cloud machine learning for feature extraction, pattern recognition, and drift compensation, lays the foundation for scalable, intelligent sensor networks that align with global sustainability and decarbonization agendas. To translate this promise into deployable technology, future work must converge algal biorefinery-scale nanoparticle production, standards for nanotoxicological risk assessment and device end-of-life management, and chip-level co-design of ZnO architectures with on-device AI accelerators for self-powered or ultralow-power environmental nodes.

## REFERENCES

1. Sharma, Mansi & Mahajan, Priyanka & Alsubaie, Abdullah & Khanna, Virat & Chahal, Surjeet & Thakur, Abhinay & Yadav, Ankush & Arya, Atul & Singh, Amanpreet & Singh, Gulab. (2024). Next-Generation Nanomaterials-based Biosensors: Real-Time Biosensing Devices for Detecting Emerging Environmental Pollutants. Materials Today Sustainability. 29. 101068. 10.1016/j.mtsust.2024.101068.
2. Popescu, S. M., “Artificial intelligence and IoT driven technologies for environmental pollution monitoring and management”, Frontiers in Environmental Science, vol. 12, Art. no. 1336088, 2024. doi:10.3389/fenvs.2024.1336088.
3. Olawade, David & Wada, Ojima & Ige, Abimbola Olufunke & Egbewole, Bamise & Olojo, Adedayo & Oladapo, Bankole. (2024). Artificial Intelligence in Environmental Monitoring: Advancements, Challenges, and Future Directions. Hygiene and Environmental Health Advances. 12. 100114. 10.1016/j.heha.2024.100114.
4. Liu, X., Lu, D., Zhang, A., Liu, Q., & Jiang, G. (2022). Data-Driven Machine Learning in Environmental Pollution: Gains and Problems. Environmental science & technology, 56(4), 2124–2133. https://doi.org/10.1021/acs.est.1c06157
5. Çaktü Güler, K., Göktürk, I., Yılmaz, F., Araz, A., & Denizli, A. (2024). Plasmonic nanosensors for environmental pollutants sensing: recent advances and perspectives. Essential Chem, 1(1), 1–19. https://doi.org/10.1080/28378083.2024.2386522
6. Chakraborty, U., Kaushik, A., Chaudhary, G. R., & Mishra, Y. K. (2024). Emerging nano-enabled gas sensor for environmental monitoring – perspectives and open challenges. *Current Opinion in Environmental Science & Health*, *37*, Article 100532. https://doi.org/10.1016/j.coesh.2024.100532
7. Fang, B., Chen, Y., Jiang, H., Liu, X., & Wang, X. (2025). Nanomaterial Engineered Biosensors and Stimulus-Responsive Platform for Emergency Monitoring and Intelligent Diagnosis. Biosensors, 15(12), 789. https://doi.org/10.3390/bios15120789
8. Nhu, V. T. T.; Dat, N. D.; Tam, L.-M.; Phuong, N. H. Beilstein J. Nanotechnol. 2022, 13, 1108–1119. doi:10.3762/bjnano.13.94
9. Ishwarya, R., Vaseeharan, B., Kalyani, S., Banumathi, B., Govindarajan, M., Alharbi, N. S., Kadaikunnan, S., Al-Anbr, M. N., Khaled, J. M., & Benelli, G. (2018). Facile green synthesis of zinc

oxide nanoparticles using Ulva lactuca seaweed extract and evaluation of their photocatalytic, antibiofilm and insecticidal activity. Journal of photochemistry and photobiology. B, Biology, 178, 249–258. https://doi.org/10.1016/j.jphotobiol.2017.11.006

10. Fouda, A., Eid, A.M., Abdelkareem, A., Said, H.A., El-Belely, E.F., Alkhalifah, D.H., Alshallash, K.S., & Hassan, S.E. (2022). Phyco-Synthesized Zinc Oxide Nanoparticles Using Marine Macroalgae, Ulva fasciata Delile, Characterization, Antibacterial Activity, Photocatalysis, and Tanning Wastewater Treatment. Catalysts.
11. Balasubramanian, R., & Ravi , S. (2023). Green Synthesised Zinc Oxide Nanoparticles from Ulva Fasciata Algae Extract for Antibacterial and Supercapacitor Application. International Journal of Membrane Science and Technology, 10(3), 3089-3099. https://doi.org/10.15379/ijmst.v10i3.3024
12. Ghosh, Tabli & Raj, Bhagya & Dash, Kshirod. (2022). A comprehensive review on nanotechnology based sensors for monitoring quality and shelf life of food products. Measurement: Food. 7. 100049. 10.1016/j.meafoo.2022.100049.
13. Adam, Tijjani. (2022). Nanosensors: Recent Perspectives on Attainments and Future Promise of Downstream Applications. Process Biochemistry. 117. 10.1016/j.procbio.2022.03.024.
14. Chaturvedi, Ambika & Tripathi, Deepti & Ranjan, Rajiv. (2025). Nano-enabled biosensors in early detection of plant diseases. Frontiers in Nanotechnology. 7. 10.3389/fnano.2025.1545792.
15. Dongfang Yang, Haowei Zheng, and Kai Wang ACS Applied Electronic Materials 2025 7 (19), 8675-8690 DOI: 10.1021/acsaelm.5c00965
16. Singh, N. B., Monjur, A., Kumar, B., Varshney, S., & Susan, M. A. B. H. (2025). Revolutionizing healthcare with nanosensor technology. RSC advances, 15(46), 38774–38810. https://doi.org/10.1039/d5ra04412j
17. Goel N, Kunal K, Kushwaha A, Kumar M. Metal oxide semiconductors for gas sensing. Engineering Reports. 2023; 5(6):e12604. doi:10.1002/eng2.12604
18. Chen, H., Chen, H., Chen, J., & Song, M. (2024). Gas Sensors Based on Semiconductor Metal Oxides Fabricated by Electrospinning: A Review. Sensors (Basel, Switzerland), 24(10), 2962. https://doi.org/10.3390/s24102962
19. Neogi, Samya & Ghosh, Ranajit. (2025). Metal-oxide gas sensors (SnO2, Fe2O3, TiO2, CoO, ZnO, NiO, CuO, and perovskite oxides). 10.1016/B978-0-443-26554-9.00012-2.
20. Franco, Mariane & Conti, Patrick & Andre, Rafaela & Correa, Daniel. (2022). A Review on Chemiresistive ZnO Gas Sensors. Sensors and Actuators Reports. 4. 100100. 10.1016/j.snr.2022.100100.
21. Sha, Rinky & Basak, Arindam & Maity, Palash & Badhulika, Sushmee. (2022). ZnO nano-structured based devices for chemical and optical sensing applications. Sensors and Actuators Reports. 4. 100098. 10.1016/j.snr.2022.100098.
22. Serrano-Lázaro, A., Portillo-Cortez, K., de la Mora Mojica, M. B., & Durán-Álvarez, J. C. (2025). A Review on ZnO Nanostructures for Optical Biosensors: Morphology, Immobilization Strategies, and Biomedical Applications. Nanomaterials (Basel, Switzerland), 15(21), 1627. https://doi.org/10.3390/nano15211627
23. Agne Sulciute, Keita Nishimura, Evgeniia Gilshtein, Federico Cesano, Guido Viscardi, Albert G. Nasibulin, Yutaka Ohno, and Simas Rackauskas, The Journal of Physical Chemistry C 2021 125 (2), 1472-1482 DOI: 10.1021/acs.jpcc.0c08459
24. Maafa I. M. (2025). Potential of Zinc Oxide Nanostructures in Biosensor Application. Biosensors, 15(1), 61. https://doi.org/10.3390/bios15010061
25. Bhakyalatha, M. & SUGUMARAN, Dr. SATHISH & Sekhar, Koppole & Silva, José P. B. & Kamakshi, Koppole. (2025). ZnO nanostructures for biosensing applications: Recent advances, challenges, and future perspectives. Microchemical Journal. 213. 113893. 10.1016/j.microc.2025.113893.
26. Bandeira, Marina & Giovanela, Marcelo & Roesch-Ely, Mariana & Devine, Declan & Crespo, Janaina. (2020). Green synthesis of zinc oxide nanoparticles: A review of the synthesis methodology and mechanism of formation. Sustainable Chemistry and Pharmacy. 15. 100223. 10.1016/j.scp.2020.100223.
27. Hussien, N. A., Khalil, M. A. E. F., Schagerl, M., & Ali, S. S. (2025). Green Synthesis of Zinc Oxide Nanoparticles as a Promising Nanomedicine Approach for Anticancer, Antibacterial, and Anti-Inflammatory Therapies. International journal of nanomedicine, 20, 4299–4317. https://doi.org/10.2147/IJN.S507214

Commented [K3]: 11 and 34 are duplicate entries

28. Rani, Nitu & Sagar, Narashans & Chauhan, Arjun & Mondal, Ankit. (2025). Green synthesis of ZnO nanoparticles: Characterization and emerging applications in sustainable agriculture. Industrial Crops and Products. 233. 10.1016/j.indcrop.2025.121393.
29. Jian Fu, Jingyi Kou, Yuxiao Han, Zekun Wang, Fan Zhang, Shanshan Sun, and Yuehui She Energy & Fuels 2025 39 (35), 16561-16594 DOI: 10.1021/acs.energyfuels.5c02453
30. Mansour, A. T., Alprol, A. E., Khedawy, M., Abualnaja, K. M., Shalaby, T. A., Rayan, G., Ramadan, K. M. A., & Ashour, M. (2022). Green Synthesis of Zinc Oxide Nanoparticles Using Red Seaweed for the Elimination of Organic Toxic Dye from an Aqueous Solution. Materials (Basel, Switzerland), 15(15), 5169. https://doi.org/10.3390/ma15155169
31. Figueira, T. , da Silva, A. , Enrich-Prast, A. , Yoneshigue-Valentin, Y. and de Oliveira, V. (2020) Structural Characterization of Ulvan Polysaccharide from Cultivated and Collected Ulva fasciata (Chlorophyta). Advances in Bioscience and Biotechnology, 11, 206-216. doi: 10.4236/abb.2020.115016.
32. Pari, R. F., Uju, U., Hardiningtyas, S. D., Ramadhan, W., Wakabayashi, R., Goto, M., & Kamiya, N. (2025). Ulva Seaweed-Derived Ulvan: A Promising Marine Polysaccharide as a Sustainable Resource for Biomaterial Design. Marine drugs, 23(2), 56. https://doi.org/10.3390/md23020056
33. Tabarsa, M., You, S., Dabaghian, E. H., & Surayot, U. (2018). Water-soluble polysaccharides from Ulva intestinalis: Molecular properties, structural elucidation and immunomodulatory activities. Journal of food and drug analysis, 26(2), 599–608. https://doi.org/10.1016/j.jfda.2017.07.016
34. Herry, Cahyana & Nurhayati, Nurhayati & Utomo, Bagus & Ardiansah, Bayu. (2017). Ulva fasciata - mediated preparation of zinc oxide nanocrystalline for one-pot multicomponent synthesis of 6-amino-3-methyl-4-phenyl-2,4-dihydropyrano[2,3-c]pyrazole-5-carbonitrile. IOP Conference Series: Materials Science and Engineering. 188. 012053. 10.1088/1757-899X/188/1/012053.
35. Al-Arjan W. S. (2022). Zinc Oxide Nanoparticles and Their Application in Adsorption of Toxic Dye from Aqueous Solution. Polymers, 14(15), 3086. https://doi.org/10.3390/polym14153086
36. Riazunnisa, Khateef & Cheemalapenta, Madhuri & Latha, A. & Nambi, Rajesh & Khadri, Habeeb & Chandrasekhar, T. & Prasanna, V. & Chandra, M.. (2024). Algae as a source of bionanofactory for the synthesis of ecofriendly nanoparticles. Environmental Nanotechnology, Monitoring & Management. 22. 101012. 10.1016/j.enmm.2024.101012.
37. Selim, Y.A., Azb, M.A., Ragab, I. et al. Green Synthesis of Zinc Oxide Nanoparticles Using Aqueous Extract of Deverra tortuosa and their Cytotoxic Activities. Sci Rep 10, 3445 (2020). https://doi.org/10.1038/s41598-020-60541-1
38. Alsaggaf, M. S., Diab, A. M., ElSaied, B. E. F., Tayel, A. A., & Moussa, S. H. (2021). Application of ZnO Nanoparticles Phycosynthesized with Ulva fasciata Extract for Preserving Peeled Shrimp Quality. Nanomaterials (Basel, Switzerland), 11(2), 385. https://doi.org/10.3390/nano11020385
39. Roshni, A. & Thambidurai, S.. (2022). Enhanced photocatalytic and antibacterial activity of ZnO with rice field crab chitosan and plectranthus amboinicus extract. Materials Chemistry and Physics. 291. 126739. 10.1016/j.matchemphys.2022.126739.
40. Ahmadzadeh, Mohammadsaleh & Norouzbeigi, Reza. (2025). Bio-templated green synthesis of ZnO nanostructures using herbal seed Mucilages: A sustainable route for dye adsorption. Chemical Physics Impact. 11. 100945. 10.1016/j.chphi.2025.100945.
41. Alprol, A.E., Eleryan, A., Abouelwafa, A. et al. Green synthesis of zinc oxide nanoparticles using Padina pavonica extract for efficient photocatalytic removal of methylene blue. Sci Rep 14, 32160 (2024). https://doi.org/10.1038/s41598-024-80757-9
42. Raza, A., Sayeed, K., Naaz, A., Muaz, M., Islam, S. N., Rahaman, S., Sama, F., Pandey, K., & Ahmad, A. (2024). Green Synthesis of ZnO Nanoparticles and Ag-Doped ZnO Nanocomposite Utilizing Sansevieria trifasciata for High-Performance Asymmetric Supercapacitors. ACS omega, 9(30), 32444–32454. https://doi.org/10.1021/acsomega.3c10060
43. A. Dumbrava, C. Matei, A. Diacon, F. Moscalu, D. Berger, Novel ZnO-biochar nanocomposites obtained by hydrothermal method in extracts of Ulva lactuca collected from Black Sea. Ceram. Int. 49(6), 10003–10013 (2023). https://doi.org/10.1016/j.ceramint.2022.11.178 DOI: 10.1016/j.ceramint.2022.11.178
44. M. Waqas Alam, A. Sharma, A. Sharma, S. Kumar, P. Mohammad Junaid, M. Awad, Electroanalysis 2025, 37, e202400246. https://doi.org/10.1002/elan.202400246

45. Al-Hashem, Mohamad & Akbar, S.A. & Morris, Patricia. (2019). Role of Oxygen Vacancies in Nanostructured Metal-Oxide Gas Sensors: A Review. Sensors and Actuators B: Chemical. 301. 126845. 10.1016/j.snb.2019.126845.
46. Farman Ullah, Khaled Ibrahim, Kissan Mistry, Abdus Samad, Ahmed Shahin, Joseph Sanderson, and Kevin Musselman ACS Sensors 2023 8 (4), 1630-1638 DOI: 10.1021/acssensors.2c02762
47. Kasumov, A. M., Korotkov, K. A., Karavaeva, V. M., Zahornyi, M. M., Dmitriev, A. I., & Ievtushenko, A. I. (2021). Photocatalysis with the Use of ZnO Nanostructures as a Method for the Purification of Aquatic Environments from Dyes. Journal of Water Chemistry and Technology, 43(4), 281–288. https://doi.org/10.3103/S1063455X21040044
48. Singh, Karanpal & Neha, & Kumar, Manish & Singh, Harbinder & Singh, Gurjinder. (2023). ZnO NPs: Photocatalytic potential, mechanistic insights, favorable parameters and challenges. Materials Today: Proceedings. 10.1016/j.matpr.2023.03.002.
49. Zhu, C., & Wang, X. (2025). Nanomaterial ZnO Synthesis and Its Photocatalytic Applications: A Review. Nanomaterials (Basel, Switzerland), 15(9), 682. https://doi.org/10.3390/nano15090682
50. Alam, U., Khan, A., Ali, D., Bahnemann, D., & Muneer, M. (2018). Comparative photocatalytic activity of sol-gel derived rare earth metal (La, Nd, Sm and Dy)-doped ZnO photocatalysts for degradation of dyes. RSC advances, 8(31), 17582–17594. https://doi.org/10.1039/c8ra01638k
51. Rojas-Forero, A. Y., Hernández-Benítez, L. Y., Ospina-Castro, M. L., Galán-Freyle, N. J., Castro-Suarez, J. R., Méndez-López, M., Hernández-Rivera, S. P., Centeno-Ortiz, J. A., Romero-Nieto, S. P., & Pacheco-Londoño, L. C. (2025). Visible-Light Photocatalytic Activity of a ZnO-Loaded Isoreticular Metal-Organic Framework. Molecules (Basel, Switzerland), 30(6), 1375. https://doi.org/10.3390/molecules30061375
52. Krasovska, M., Gerbreders, V., Mihailova, I., Ogurcovs, A., Sledevskis, E., Gerbreders, A., & Sarajevs, P. (2018). ZnO-nanostructure-based electrochemical sensor: Effect of nanostructure morphology on the sensing of heavy metal ions. Beilstein journal of nanotechnology, 9, 2421–2431. https://doi.org/10.3762/bjnano.9.227
53. A. Belcovici, C. I. Fort, L. E. Mureşan, I. Perhaiţa, G. Borodi, G. L. Turdean, Electroanalysis 2023, 35, e202200395.
54. Dessie, Y., Ravikumar, R. C., Khasim, S., Somashekar, M. N., Tufa, L. T., Abraham Tesfaye, G., Tilahun Bekele, E., & Leku, D. T. (2025). Biosynthesized ZnO/Co3O4 Nanocomposite-Modified Electrode for Electrocatalytic Lead Detection and Quantification. ACS omega, 10(50), 62268–62281. https://doi.org/10.1021/acsomega.5c10161
55. Ismardi, A., Gunawan, T. D., Suhendi, A., & Fathona, I. W. (2024). Study of graphene incorporation into ZnO-PVA nanocomposites modified electrode for sensitive detection of cadmium. Heliyon, 10(11), e31565. https://doi.org/10.1016/j.heliyon.2024.e31565
56. Jangra, Vikas & Kaur, Harpreet & Kumar, Narvdeshwar & Ratnam, Anand & Prasad, L.B. & Sonkar, Piyush. (2025). Advanced ZnO-g-C3N4 nanocomposite: A highly sensitive electrochemical sensor for simultaneous determination of lead and mercury ions. Solid State Sciences. 170. 108116. 10.1016/j.solidstatesciences.2025.108116.
57. Liu, Meihui & Ren, Ruirui & Zhou, Xinyuan & Zhu, Shan & Wang, Tie. (2025). From gas sensing to AI-gas sensing. Chemical Communications. 61. 10.1039/D5CC01291K.
58. Peresi Majura Bulemo, Dong-Ha Kim, Hamin Shin, Hee-Jin Cho, Won-Tae Koo, Seon-Jin Choi, Chungseong Park, Jaewan Ahn, Andreas T. Güntner, Reginald M. Penner, and Il-Doo Kim Chemical Reviews 2025 125 (8), 4111-4183 DOI: 10.1021/acs.chemrev.4c00592
59. Park, Jaebum & Same, Noel & Yakub, Abdulfatai & Lim, Jeong & Roh, Jong & Huh, Jeung-Soo. (2024). Formaldehyde Gas Response and Selectivity of ZnO-SnO2 Gas Sensors. Sensors and Actuators B: Chemical. 425. 136958. 10.1016/j.snb.2024.136958.
60. Kwon, Yeongmin & Son, Yeseul & Lee, Do & Min Hyeok, Lim & Han, Jin Kyu & Jang, Moonjeong & Park, Seoungwoong & Kang, Saewon & Yim, Soonmin & Myung, Sung & Lim, Jongsun & Lee, Sun & Bae, Garam & Kim, Seong & Song, Wooseok. (2025). Enhancing selectivity and sensitivity in gas sensors through noble metal-decorated ZnO and machine learning. Applied Surface Science. 693. 162750. 10.1016/j.apsusc.2025.162750.

61. Ren, W., Zhao, C., Niu, G., Zhuang, Y. and Wang, F. (2022), Gas Sensor Array with Pattern Recognition Algorithms for Highly Sensitive and Selective Discrimination of Trimethylamine. Adv. Intell. Syst., 4: 2200169. https://doi.org/10.1002/aisy.202200169
62. Yu, Y., Cao, X., Li, C., Zhou, M., Liu, T., Liu, J., & Zhang, L. (2025). A Review of Machine Learning-Assisted Gas Sensor Arrays in Medical Diagnosis. Biosensors, 15(8), 548. https://doi.org/10.3390/bios15080548
63. Z S Chen, Z Chen, Z L Song, W H Ye, Z Y Fan, Smart gas sensor arrays powered by artificial intelligence[J]. J. Semicond., 2019, 40(11): 111601. doi: 10.1088/1674-4926/40/11/111601.
64. Vergara, Alexander & Vembu, Shankar & Ayhan, Tuba & Ryan, Margaret & Homer, M.L. & Huerta, Ramón. (2012). Chemical gas sensor drift compensation using classifier ensembles. Sensors and Actuators B: Chemical. s 166–167. 320–329. 10.1016/j.snb.2012.01.074.
65. Arrojo, Markel & Cejudo, Ander & Gutiérrez, Miriam & Paolini, Giovanni & Haick, Hossam & Maiza, Mikel & Martín, Cristina. (2025). AI-enhanced spatio-temporal volatile organic compound profile characterization integrated with GIS for environmental monitoring using Spectrometer-On-Card. Journal of Hazardous Materials Advances. 19. 100765. 10.1016/j.hazadv.2025.100765.
66. Liu, H., Chu, R., & Tang, Z. (2015). Metal oxide gas sensor drift compensation using a two-dimensional classifier ensemble. Sensors (Basel, Switzerland), 15(5), 10180–10193. https://doi.org/10.3390/s150510180
67. Du, M., Abdulraheem, M.I., Xu, L. et al. Enhanced Selectivity Electronic Nose Systems for Agricultural Ammonia Gas Detection via a co-designed WO3-ZnO Sensor Array and Convolutional Neural Networks. Sci Rep 15, 39100 (2025). https://doi.org/10.1038/s41598-025-26084-z
68. Singh, S., S, S., Varma, P., Sreelekha, G., Adak, C., Shukla, R. P., & Kamble, V. B. (2024). Metal oxide-based gas sensor array for VOCs determination in complex mixtures using machine learning. Mikrochimica acta, 191(4), 196. https://doi.org/10.1007/s00604-024-06258-8
69. Yan J., Kang Y., Wang T., et al. (2025). AI empowers intelligent chemical sensing systems. The Innovation Informatics 1:100014. https://doi.org/10.59717/j.xinn-inform.2025.100014
70. Luo, W., Dai, F., Liu, Y. et al. Pulse-driven MEMS gas sensor combined with machine learning for selective gas identification. Microsyst Nanoeng 11, 72 (2025). https://doi.org/10.1038/s41378-025-00934-2
71. Feng Y, Wang Y, Beykal B, Qiao M, Xiao Z, Luo Y (2024) A mechanistic review on machine learning-supported detection and analysis of volatile organic compounds for food quality and safety. Trends Food Sci Technol 143:104297. https://doi.org/10.1016/j.tifs.2023.104297 DOI: 10.1016/j.tifs.2023.104297
72. Aliyana, A.K., Naveen Kumar, S.K., Marimuthu, P. et al. Machine learning-assisted ammonium detection using zinc oxide/multi-walled carbon nanotube composite based impedance sensors. Sci Rep 11, 24321 (2021). https://doi.org/10.1038/s41598-021-03674-1
73. Nguyen, Ngoc-Viet & Phuoc, Phan Hong & Thong, Le & Nguyen, Chien & Hieu, Nguyen. (2024). A Comparative Study of Machine Learning Models for Identifying Noxious Gases through Thermal Fingerprint Measurements and MOS Sensors. Sensors and Actuators A: Physical. 375. 115510. 10.1016/j.sna.2024.115510.
74. Souissi, R., Bouricha, B., Bouguila, N., El Mir, L., Labidi, A., & Abderrabba, M. (2023). Chemical VOC sensing mechanism of sol-gel ZnO pellets and linear discriminant analysis for instantaneous selectivity. RSC advances, 13(30), 20651–20662. https://doi.org/10.1039/d3ra03042c
75. Kanaparthi, S., & Singh, S. G. (2021). Reduction of the Measurement Time of a Chemiresistive Gas Sensor Using Transient Analysis and the Cantor Pairing Function. ACS measurement science au, 2(2), 113–119. https://doi.org/10.1021/acsmeasuresciau.1c00043
76. Heng, Yuanli & Zhou, Yangming & Duc Hoa, Nguyen & Duy, Nguyen & Jiao, Mingzhi. (2025). An electronic nose drift compensation algorithm based on semi-supervised adversarial domain adaptive convolutional neural network. Sensors and Actuators B: Chemical. 422. 136642. 10.1016/j.snb.2024.136642.
77. Lin, Juntao & Zhan, Xianghao. (2025). Sensor Drift Compensation in Electronic-Nose-Based Gas Recognition Using Knowledge Distillation. 10.48550/arXiv.2507.17071.
78. Jiang, K., Zeng, M., Wang, T., Wu, Y., Ni, W., Chen, L., Yang, J., Hu, N., Zhang, B., Xuan, F., Li, S., Shi, A., & Yang, Z. (2025). Gas Sensor Drift Compensation Using Semi-Supervised Ensemble

Classifiers with Multi-Level Features and Center Loss. ACS sensors, 10(4), 2906–2918. https://doi.org/10.1021/acssensors.4c03655
79. Zhang, Y., Yan, J., Wang, Z., Peng, X., Tian, Y., & Duan, S. (2021). TDACNN: Target-domain-free Domain Adaptation Convolutional Neural Network for Drift Compensation in Gas Sensors. ArXiv, abs/2110.07509.
80. Zhu, J., Zhan, Y., Ni, X., & Gao, Y. (2025). Artificial Intelligence of Things in Hydrogen Sensing: Toward Optic and Intelligent System. Research (Washington, D.C.), 8, 0750. https://doi.org/10.34133/research.0750
81. Preeti, Km & Kumar, Anirudh & Jain, Naini & Kaushik Fics Fgan Mrsc Ecs Acs Aaas, Ajeet & Mishra, Yogendra & Sharma, Sanjeev. (2023). Tailored ZnO nanostructures for efficient sensing of toxic metallic ions of drainage systems. Materials Today Sustainability. 24. 100515. 10.1016/j.mtsust.2023.100515.
82. Roostaei, J., Wager, Y. Z., Shi, W., Dittrich, T., Miller, C., & Gopalakrishnan, K. (2023). IoT-based Edge Computing (IoTEC) for Improved Environmental Monitoring. Sustainable computing : informatics and systems, 38, 100870. https://doi.org/10.1016/j.suscom.2023.100870
83. Abdelkarem, K., Saad, R., El Sayed, A. M., Fathy, M. I., Shaban, M., & Hamdy, H. (2023). Design of high-sensitivity La-doped ZnO sensors for CO2 gas detection at room temperature. Scientific reports, 13(1), 18398. https://doi.org/10.1038/s41598-023-45196-y
84. Keerthana, S & Kailasam, Rathnakannan. (2022). Room temperature operated carbon dioxide sensor based on silver doped zinc oxide/cupric oxide nanoflowers. Sensors and Actuators B: Chemical. 378. 133181. 10.1016/j.snb.2022.133181.
85. Salimian, Firouzeh & Hemmati, Alireza & Ghaemi, Ahad. (2025). A review of nanostructured carbon dioxide sensors based on electrical and thermal conductivity. Results in Engineering. 26. 105633. 10.1016/j.rineng.2025.105633.
86. Asad, Hira, Ahmed, Tanveer, Naz, Huma, Abbas, Khalid, Latif, Fariha, Suleman, Saba, Habib, Rana Zeeshan, Bashir, Zainab, Rizwan, Muhammad Tayyeb, Iqbal, Rashid, Swelum, Ayman A., Impact of Green-Synthesized Zinc Oxide Nanoparticles (ZnO NPs) on the Biochemical and Histological Profiles of Cyprinus carpio, Aquaculture Research, 2025, 5327177, 10 pages, 2025. https://doi.org/10.1155/are/5327177
87. Zavitri, N.G., Syahbaniati, A.P., Primastuti, R.K., Putri, R.M., Damayanti, S., & Wibowo, I. (2023). Toxicity evaluation of zinc oxide nanoparticles green synthesized using papaya extract in zebrafish. Biomedical Reports, 19, 96. https://doi.org/10.3892/br.2023.1678
88. Ragavendran, Chinnasamy & Kamaraj, Chinnaperumal & Alrefaei, Abdulwahed & Arumugam, Priyadharsan & Matos, Letícia & Malafaia, Guilherme & Moulishankar, Anguraj & Rajan, Sundar. (2024). Green-route synthesis of ZnO nanoparticles via Solanum surattense leaf extract: Characterization, biomedical applications and their ecotoxicity assessment of zebrafish embryo model. South African Journal of Botany. 167. 10.1016/j.sajb.2024.02.049.
89. Nasim, I., Ragavendran, C., Kamaraj, C., Almutairi, H. H., Alam, M. W., Manimaran, K., & Nakouti, I. (2024). Green synthesis of ZnO nanoparticles and biological applications as broad-spectrum bactericidal, antibiofilm effects and biocompatibility studies on Zebrafish embryo. Inorganic Chemistry Communications, 169, 113049.
90. Ramaraj, N., Thiripuranathar, G., Ekanayake, S., Attanayake, K., & Marapana, U. (2025). Phyco-synthesized inorganic nanoparticles and their biomedical applications. RSC Sustainability, 3(6), 2567-2581.
91. Tian, Shuo & Li, Bin & Dai, Ye-Jing & Wang, Zhong. (2023). Piezo-phototronic and pyro-phototronic effects enhanced broadband photosensing. Materials Today. 68. 10.1016/j.mattod.2023.07.001.
92. Zhang, Z., Liu, X., Zhou, H., Xu, S. and Lee, C. (2024), Advances in Machine-Learning Enhanced Nanosensors: From Cloud Artificial Intelligence Toward Future Edge Computing at Chip Level. Small Struct., 5: 2300325. https://doi.org/10.1002/sstr.202300325
93. Jiaqing Zhu, Lechen Chen, Wangze Ni, Weiwei Cheng, Zhi Yang, Shusheng Xu, Tao Wang, Bowei Zhang, and Fuzhen Xuan ACS Sensors 2025 10 (4), 2531-2541 DOI: 10.1021/acssensors.4c02789